Advances in Electrospun Composite Polymer/Zeolite and Geopolymer Nanofibers:

A Comprehensive Review

Mariana Schneider[1,2], Enrique Rodríguez-Castellón[2], M. Olga Guerrero-Pérez[2], Dachamir Hotza[1], Agenor De Noni Junior[1], Regina de Fátima Peralta Muniz Moreira[1]*

[1] Department of Chemical Engineering and Food Engineering, Federal University of Santa Catarina, 88040-900 Florianópolis, SC, Brazil

[2] Departments of Inorganic Chemistry and Chemical Engineering, Faculty of Sciences, University of Málaga, Spain

* Corresponding author: regina.moreira@ufsc.br

ABSTRACT

Electrospinning is widely recognized as an efficient, simple, and cost-effective technique for producing nanofibers. It has successfully led to the fabrication of various ultrafine polymer composites. This method has spurred extensive research in fields such as medicine, electronics, chemistry, and physics, where producing materials via electrospinning is very promising for revolutionizing many fields. This paper presents a comprehensive review of the latest research and developments on electrospun composite polymer/zeolite nanofibers and geopolymers. The study examines processing, structure, characterization, and potential applications. Detailed information on these composites, including their specific electrospinning conditions, has been thoughtfully summarized in this work. Furthermore, we address important concerns related to the technology's limitations and existing research challenges. In the studies analyzed, a diverse range of polymers was employed, the most frequent were polyvinyl alcohol, polycaprolactone, and polylactic acid. The applications of zeolite/polymer composites were equally varied, encompassing fields such as catalysis, filtration, adsorption, and pesticide residue analysis in food samples. Moreover, these composites were found to be useful in the medical sector, including applications in dental tissue engineering and for treating bacterial infections.

Keywords: electrospinning, polymer composites, nanofibers, zeolite, geopolymers.

1. INTRODUCTION

Zeolitic materials, and their applications in adsorption, catalysis, and ion exchange have been extensively investigated during the last decades. There are 250 different types of zeolites, 46 are natural, and 204 synthetic [1,2]. Some of the zeolite types have great importance in industrial studies and applications like separation processes, chemical synthesis, and sensor devices [3]. The precursor most used for zeolite synthesis is kaolin. Moreover, natural aluminosilicate minerals and industrial solid waste materials, including fly ash, metakaolin, coal gangue, rice husks, diatomite, and even geopolymers, have been investigated as viable sources of raw materials in the synthesis of zeolites [4–7]. These raw materials are typically combined with an alkaline activator, such as sodium silicate, sodium hydroxide, or potassium disilicate, to facilitate the zeolite synthesis process [1,8].

Geopolymers are amorphous three-dimensional aluminosilicate materials, classified as inorganic polymers that have ceramic-like properties and are produced and hardened at ambient temperature. Recently, the synthesis of geopolymeric materials has emerged as a promising way to recycle solid industrial byproducts due to their environmentally friendly attributes. This is particularly relevant for various waste streams, including debris from civil construction and powdered waste from ground bricks [9], coconut ash [10], fly ash, rice husk ash, phosphate waste [5,11], slag, pozzolan, clay, kaolinite [12], and metakaolin/metakaolinite [5,13–16]. In addition, geopolymers offer diverse applications, including their use in thermal insulation [17], self-cleaning concrete cementation [18], CO_2 adsorption [19–21], foam concrete [9], ceramic foam [13], arsenic removal from groundwater [14], construction materials [22–24].

Various methods are available for manufacturing such materials, with recent advances notably focusing on zeolitic composites and the preparation of geopolymeric materials. These methods include: 3-dimensional printing [22], reactive emulsification

[14], extrusion [15], polymeric molding [13], microwave heating [11] for geopolymeric materials and 3-dimensional printing [25], heat mixing [1], co-extrusion [26], and the phase-inversion technique [27] for zeolite/polymer composites.

A standout among these methods is the electrospinning technique, known for its simplicity and cost-effectiveness in producing nanofibers from various polymer sources. This technique consists of forming fibers from a polymer solution, ejecting them from a fine spinneret between two electrodes bearing electrical charges of opposite polarity, one placed on the spinneret and the other on a collector. The charged solution jet evaporates during its travel towards the collector to form the nonwoven fibers' arrangement [28–30].

The characteristics of the electrospinning solution, such as surface tension, electrical conductivity, volatility, and solvent viscosity, along with operational variables such as applied voltage; collector distance and solution flow rate, and environmental factors like humidity and temperature, can collectively influence the properties of the fibers. These factors highlight that by modifying fluid properties, it is possible to produce various types of fibers as needed [28,31,32].

Moreover, the diameter of the nanofibers can be changed by using different concentrations of solutions and electrical voltage. Thus, by adjusting the electrospinning, calcination settings, and precursor compositions, customized architectures may be created, such as hollow, porous, core-shell, and helical fibers [33,34]. Increasing viscosity tends to promote the formation of fibers by extending the electrospun fiber, while lower viscosity can result in the formation of beads rather than continuous fibers [35]. Furthermore, some parameters such as the distance between electrodes, applied voltage, humidity, volumetric flow, and needle diameter can be adjusted to allow sufficient solvent evaporation, preventing the fibers from melting, or even from being formed [27].

Despite being a relatively recent technique, there is a substantial body of literature that employs the electrospinning method to create diverse materials for use in a wide array of fields. For example, this method has been applied in the development of controlled-release vitamin C capsules [30], and in consumer products such as car filters, face masks, and water filters [35], and in some of the applications of zeolite/polymer and/or geopolymer/polymer composites studied in the literature are desalination [36], filtration and dehumidification [38], medicine [39–41] insecticide detection [42], biofilms [43], catalysts [44], and adsorption [45], and more applications will be presented below.

2. ADVANCES IN ELECTROSPINNING TECHNOLOGY

The first concept of electrospinning was designed in 1600 in a study by William Gilbert, in which he observed the formation of a cone-shaped water droplet in the presence of an electric field [35]. In 1747, an electrospray experiment was carried out by Abbe Nollet, and the work demonstrated that water could be sprayed as an aerosol when passing through an electrostatically charged vessel [46]. However, the behavior of the charged droplets was only systematically studied in 1882, by Lord Rayleigh, who theoretically estimated the number of charges that a droplet could carry before the liquid is ejected from a surface [47].

The electrospinning technique can be viewed as a variation of electrospraying, as both methods rely on high voltage to expel liquid jets. However, the key distinction between them hinges on the viscosity and viscoelasticity of the liquid used, as well as the behavior of the jet [35]. In electrospinning, the jet can be continuous, resulting in fiber production, while in electrospraying, the liquid jet breaks into droplets, forming particles (Figures 1 and 2). In 1902, John Cooley and Willian Morton patented the first two types of electrospinning equipment [48,49]. In 1934 and 1944, Anton Formhals patented an

improved electrospinning device, which led to the commercialization of the equipment for textile fabrication [50,51].
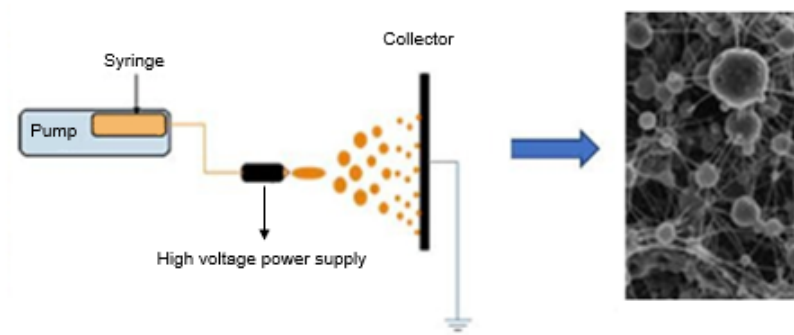

Figure 1. Schematic diagram of the electrospraying setup and SEM images of oil-loaded capsules (adapted from Rahmani-Manglano et al., 2024). Copyright © 2024 Nor E. Rahmani-Manglano, et al.
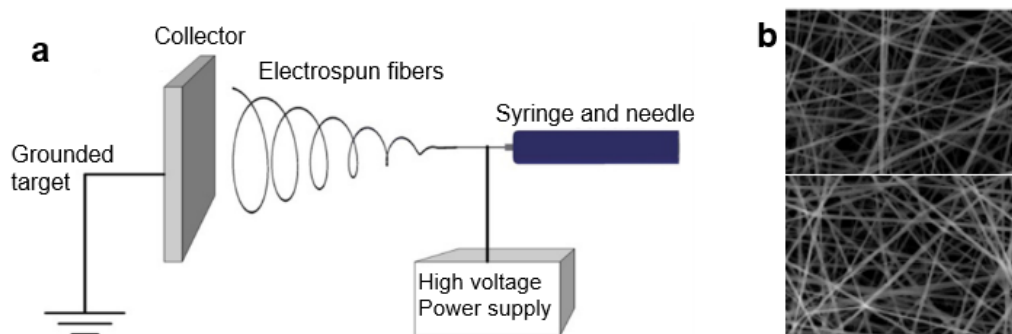

Figure 2. Schematic diagram of the electrospinning setup (a) and SEM images of electrospun lignin-zeolite nanofibers (b) (adapted from Bahi et al., 2017). Copyright © 2017 Addie Bahi, et al.

The use of electrospinning to produce nanofibers was first applied in 1938 when air filters were produced for capturing aerosol particles, and this work led to the manufacture of gas masks using nanofiber-based mats for smoke filters [35]. However, the understanding of the mechanics of electrospinning was developed only between 1964 and 1969, when Geoffrey Taylor published papers showing how to mathematically describe and model the change from a spherical to a conical shape of a polymer solution or molten droplet under the influence of a strong electric field [52–54].

Progress in electrospinning remained relatively dormant until between 1999 and 2001, when research groups collectively showed that various organic polymers could indeed be electrospun into nanofibers [31,55–58]. It was during this period that multiple research teams revitalized the technique, thanks to the availability of electron microscopes capable of nanoscale observation [35].

At the beginning of this century, electrospinning methods and equipment began to receive more attention and improvements. As has been established, the ability to introduce novel materials and formulations facilitates the production of composite and ceramic nanofibers, opening new avenues for applications in catalysis, energy conversion, harvesting, and storage. Moreover, the structure control and alignment of electrospun nanofibers were also studied, and methods for combining different properties such as size, structure, composition, morphology, porosity, and assembly of nanofibers were developed, increasing the range of applications [35].

The electrospinning equipment consists of a syringe filled with a polymer solution, connected to a piston to control pressure and flow rate. The syringe needle, connected to an adjustable power source, is set to a specific voltage. With a separation between the needle's nozzle and the collector, electrospinning employs an electrical charge to draw fine fibers from solution droplets. The high voltage induces charge, counteracting droplet surface tension and creating a fine jet. The jet diameter decreases as it reaches the collection target [83]. The production of nanofibers with diversified compositions, structures (hollow fibers, porous, core-shell, helical fibers, etc), and properties were recently revised by Xue et al. [35]. However, the addition of porous materials enables new applications for these materials, since it explores adsorptive and catalytic properties.

Figure 3 illustrates a typical example of electrospun nanofibers that were produced by the physical cross-linking of poly(3,4-ethylenedioxythiophene) (PEDOT) and poly(styrenesulfonate) (PSS) by Mg^{2+} ions for the improvement of viscoelasticity, and a photograph of the nanofibers during the electrospinning process.
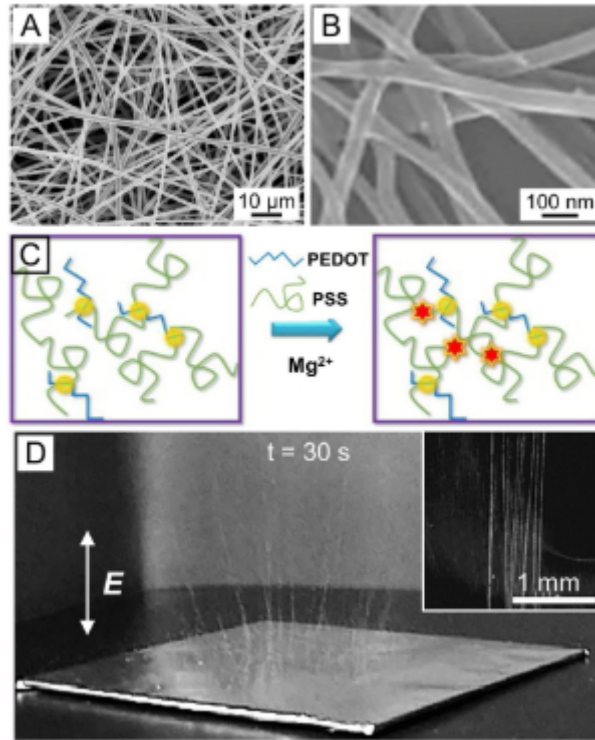

Figure 3. SEM images of the electrospun nanofiber (A and B), schema of the physical cross-linking of PEDOT and PSS by Mg^{2+} (C), and a photograph of the nanofibers during the electrospinning process (D) (Xue et al., 2019).

A recent development has brought forth a highly adaptable x-y-z electrospinning apparatus for nanofiber synthesis. This innovative equipment has been characterized as a versatile system designed for the large-area, high-precision deposition, writing, and printing of electrospun nanofibers, and it essentially functions like a 3D printer [30]. Figure 4 provides a visual representation of this apparatus, highlighting its capacity for precise, rapid, and independent x-y-z movement.
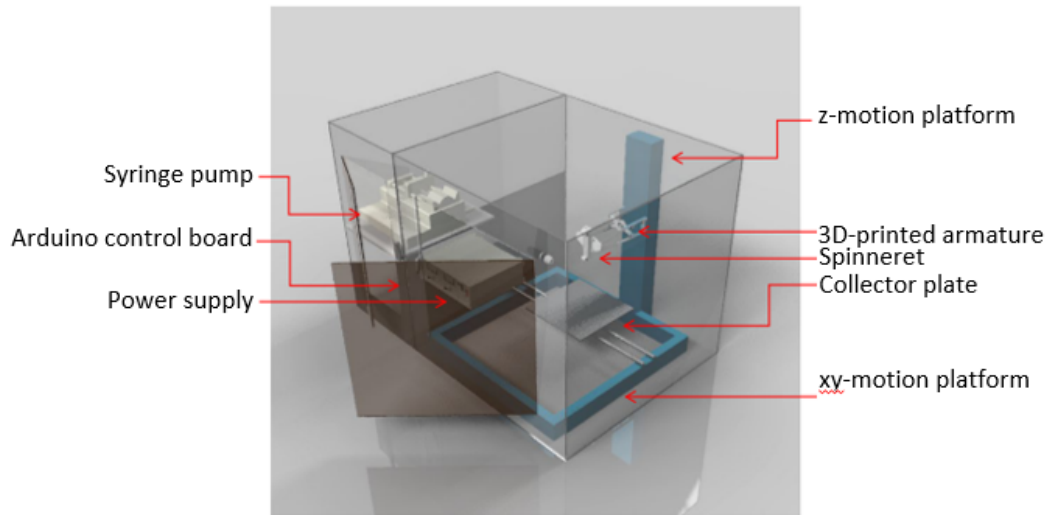
Figure 4. Illustration of an x–y–z electrospinning device (Calzado-Delgado et al., 2022).

Furthermore, the device incorporates precise control over the electric field, ensuring not only the controlled fiber deposition but also the regulation of fiber diameter and size. These attributes contribute to making the final material highly reproducible, a valuable feature for industrial-scale production [30]. Finally, Figure 5 illustrates the difference between the membrane obtained through a traditional and using the x–y–z electrospinning device, both carried out with the same solution, and parameters, at 0.1 mL/h flow; 7.3 kV, and spinneret height (z) of 11 cm [30]. The fundamentals and parameters most used to produce zeolite/polymer, and geopolymer/polymer membranes are discussed in the following sections.
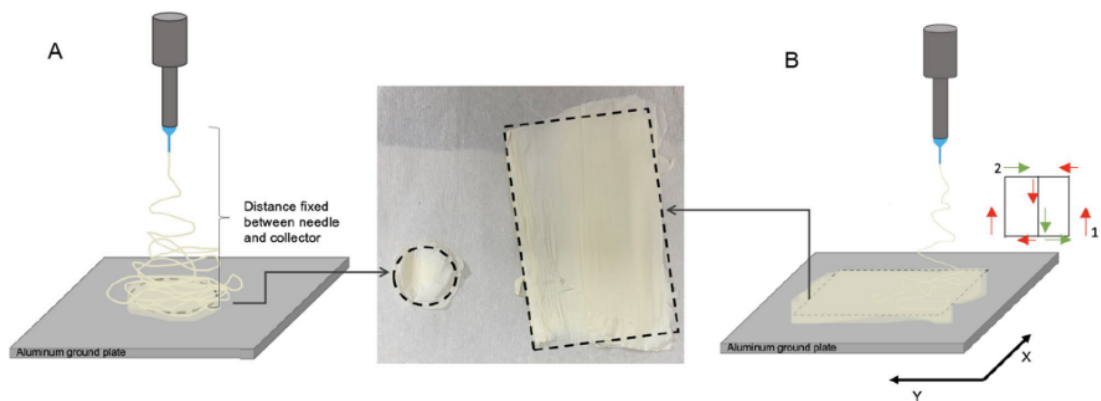
Figure 5. Illustration of the membranes obtained through (A) the conventional and (B) the x–y–z electrospinning device (Calzado-Delgado et al., 2022).

3. ZEOLITES IN ELECTROSPUN COMPOSITES

Zeolites have firmly established themselves as a prominent subject in the literature, with a focus on both their synthesis and diverse applications. The synthesis of zeolites typically involves using well-defined saturated aqueous solutions, within specific compositions and under controlled temperature and pressure conditions. Consequently, manipulating the composition and operational parameters of the synthesis gel allows producing zeolites with varying structural features and chemical compositions. The hydrothermal/hydrogel method remains the primary technique used in the production of zeolites. Furthermore, it is the most suitable method for large-scale synthesis [1,59,60]. Alternative methods for producing zeolite/polymer composites are 3-dimensional printing [25], heat mixing [1], co-extrusion [26], and the phase-inversion technique [61].

Shaping zeolites through electrospinning is a relatively emerging field, with limited literature dedicated to the production of zeolite/polymer composites. This is because polymers are the predominant base for materials obtained via electrospinning. Furthermore, in some instances, zeolites are not the primary component but rather serve as an integral part of the polymer structure.

Regarding porous geopolymers, numerous techniques are available for producing them, such as chemical foaming [9], the lyophilization technique [21], polymeric molding [13], microwave heating [11], direct ink-printing [62], the mixed foam method [10], reactive emulsion [14], extrusion [15], and 3D printing [22,24,63–66].

In this context, in relation to preparing zeolite/polymer composites through the electrospinning process, polycaprolactone (PCL) is the most frequently utilized polymer. It is closely followed by-polyvinylpyrrolidone (PVP) and polylactic acid (PLA). In some instances, a combination of two polymers is employed. Table 1 provides an overview of

various applications and compositions of electrospun zeolitic composites as reported in recent literature.

Table 1. Electrospun polymeric composites with zeolite fillers and their respective applications.

Zeolite (filler)	Polymeric (matrix)	Additive	Solvent (Electrospinnable base liquid)	Application	Reference
Zeolite	Polyvinyl alcohol (PVA)	Citric acid	Water	Ni^{2+} and Cd^{2+} removal from aqueous solution	[67]
Zeolite-Y (600nm-1μm)	Polyvinylpyrrolidone (PVP)	-	Ethanol	Catalysis	[68]
Zeolite (<45μm)	Polyvinylidene fluoride (PVDF)	-	Dimethylformamide (DMF), acetone	Filtering and dehumidification	[38]
NaY zeolite (0.75μm)	PVP	-	Ethanol	Benzene adsorption	[45]
Zeolite (1-3μm)	Polycaprolactone (PCL)	Silica (~17 μm)	Chloroform, butanol	Histamine-binding	[69]
Copper salt ion-exchange zeolite	Polylactic acid (PLA)	Cellulose nanofibers	Acetone, acetic acid, acetic anhydride, tartaric acid	Antimicrobial barrier	[43]

nanoparticles (~43.73nm)					
Zeolite (~2μm)	PCL, PLA	Nano-hydroxyapatite (nHA)	Dichloromethane (DCM): methanol	Dental tissue engineering	[70]
Zeolite imidazole framework-8 (ZIF-8)	PLA	Titanium carbide (MXene)	DCM, ethanol	Bacterial infections	[41]
ZSM-5 zeolite (2078.79nm), beta Zeolite (842.06nm)	PVA, polyethersulfone (PES)	-	DMF, acetone	Creatinine adsorption	[71]
Zeolite	PS	-	DMF	Desalination	[36]
HZSM-5 zeolite	PVP	Zirconium acetate	Acetic acid	Catalysis (dimethyl ether-to-olefins process)	[44]

Zeolite NaX	PVDF, Polyacrylonitrile (PAN), Polydopamine (PDA)	-	DMF, acetone	Adsorption/separation membranes in organic carbon interception, Ammonium recovery	[72]
Zeolite Y (90 - 100nm)	PCL, Gelatin	Curcumin	Acetic acid, formic acid	Postsurgical glioblastoma treatment	[73]
Zeolitic-based metal-organic frameworks	Styrene acrylonitrile copolymer	Chitosan	Dimethyl sulfoxide	Pesticide residue analysis in food samples	[74]
ZSM-5 zeolite	PCL, polyethylene glycol	Dexamethasone, and ascorbic	DCM, methanol	Dexamethasone and and ascorbic acid delivery for bone regeneration	[40]

4. GEOPOLYMERS IN ELECTROSPUN COMPOSITES

To the best of our knowledge, there is only one reported study in the literature which explores the utilization of electrospinning in the context of geopolymer development [37]. In this study, Tang et al. showed the feasibility of creating resilient geopolymer composites. They achieved this by combining the electrospinning process with the sol-gel method, resulting in the production of elastic nanofibers capable of withstanding high temperatures.

Electrospinning can be used to prepare geopolymer samples from a mixture of aluminiferous, siliceous, and phosphoric acid. In the study carried out by Tang et al. [37] at first, a stabilizer solution (mixing boric acid, absolute ethanol, tetraethyl orthosilicate (TEOS), and deionized water) was mixed with aluminum nitrate nonahydrate under reflux. Then, PVA was added and continuously stirred until it was completely dissolved, forming a spinnable solution. The geopolymer solution was then suctioned into a syringe using a syringe needle. The solution was then fed at a controlled propulsion velocity of 1 mL/h, and electrospun with a voltage of 12 kV and receiving distance of 15 cm. After the spinning process, the nanofibers were collected by a rotating drum and very highly and continuously aligned in a single direction. The nanofibers had high tensile strength along the axial direction but extremely low strength limits in the radial direction. For this reason, the fibers were cut from the rotating drum collector and gathered as mats, layer by layer. Finally, the multi-layered mats were compacted in a hydraulic press at a pressure of 50–100 MPa to obtain an isotropic elastic nano geopolymer [37]. A schema of the procedure and final sample is presented in Figure 6.
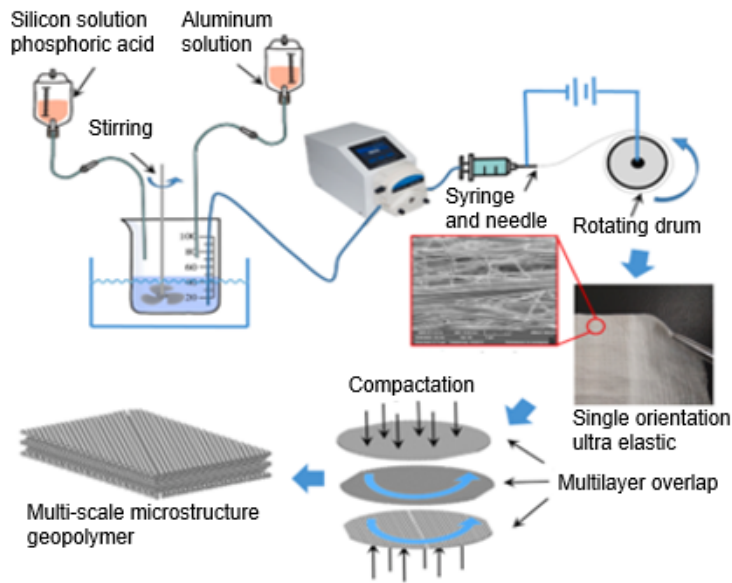
Figure 6. Schematic diagram of the electrospinning of geopolymer-based fibers (adapted from Tang et al., 2022). Copyright © 2022 Jiabo Tang, et al.

The electrospinning method created a lamellar-structured elastic geopolymer with a multi-scale microstructure (Figure 6). Some of the characteristics, like elemental composition, crystallinity, and oxide analysis, were analyzed. The electrospun geopolymer presented elemental composition peaks of Si, Al, and P, the Si:Al molar ratio was set as 1.5:1, and the diameter ratio of the nanofiber was around 500 nm. The crystallinity showed that the geopolymer is amorphous and the oxide analysis showed the characteristic peaks of aluminosilicates, polyphosphates, and silicophosphates. [37]

Finally, according to the authors, the advantages of this design were that the geopolymer retained its excellent mechanical properties and gained the benefits of unique thermal and corrosion stability. The multi-scaled, micro-structured geopolymer exhibited isotropic elasticity, demonstrated complete recovery from large deformations, and had high chemical and fire resistance properties since the electrospun nano-geopolymer displayed temperature-invariant super elasticity over 600 ºC.

5. POLYMER SELECTION IN ELECTROSPUN ZEOLITE COMPOSITES

This section will detail the preparation methods for a selection of samples listed in Table 1, with a focus on the rationale behind polymer choice. As mentioned above, diverse polymers have been employed to prepare zeolite-based composites through the electrospinning process. This section will shed light on the specific polymer selections and their relevance to the manufacturing process.

Kang and Kang [38] developed a zeolite/PVDF composite for application in filtration and dehumidification simultaneously using the electrospinning technique. To produce the composite, 12 wt% of PVDF powder (Mw ~531,000) was dissolved in dimethylformamide and acetone in a 3:7 volume ratio, then the zeolite powder (<45 μm) was added to the solution, which in this case was used as a desiccant material. Then, the zeolite/PVDF solutions were treated with ultrasonication to disperse the zeolite particles for 48 h at 35°C. PVDF was chosen as a polymer due to its outstanding thermal stability, mechanical strength, chemical resistance, piezoelectric property, and lower weight than other polymers, which are important characteristics for filter application. Moreover, Kang and Kang [38] pointed out that electrospun PVDF nanofiber film shows improved physical properties, like tensile stress and tensile modulus, by thermal and oxygen plasma treatments.

According to Sihombing et al. [36], polystyrene (PS) has several interesting characteristics. It is low cost, non-degradable, and has high mechanical strength, although the hydrophobic properties limit its application as a membrane for water treatment. This limitation still offers an advantage since water molecules can pass through the membrane when the breakthrough pressure is attained, moreover, the use of zeolite as a nanofiller can enhance the hydrophilicity of polystyrene membranes, forming a composite suitable for water filtration. Thus, they developed a novel composite membrane of PS integrated

with natural zeolite particles for desalination purposes. To do so, first, 6 wt% of zeolite powder was dispersed in sulfuric acid and stirred at 350 rpm, and 70 °C for 4 h. The residue obtained was then washed until neutral pH was reached, and the material was dried at 105 °C for 1 h. The membrane was prepared by dissolving 4.7 g of PS in 20 ml of dimethylformamide and stirring at 350 rpm, 80 °C for 30 min. Finally, the zeolite microparticles were added to the solution.

Rad et al. [67] produced a PVA/zeolite nanofibrous adsorbent for the removal of Ni^{2+} and Cd^{2+} from water. To prepare the solution, first, the solution containing 10% of PVA in DIW was refluxed at 80 °C for 4h, then the zeolite was added to the PVA solution. Lastly, citric acid was added to the solution at a weight of 10% of the total solution and mixed at 20 °C for 5h. In this case, PVA polymer was chosen due to its high potential for loading nanoparticles without compromising mechanical stability. PVA and polyacrylamide have been the most used polymers to produce zeolite-based composite fibers, due to their low cost, low toxicity, good tensile strength, biocompatibility, and excellent hydrophilicity [45].

Lastly, Haghdoost et al. [71] produced a PES/PVP-zeolite core-shell composite nanofiber. To do so, they prepared two solutions, PVP/zeolite (shell) and PES (core). The PES solution was prepared by dissolving 25% (v/v) of PES flakes in DMF at room temperature for 3h. The PVP/zeolite solution was prepared by dissolving 10% PVP powder in acetone for 12h, then the zeolites (at 10 and 20 wt%) were directly added to the PVP solution and stirred at room temperature for 24h. Finally, the dispersions were sonicated for 1h before the electrospinning process.

Regarding the characteristics of the fluid for production by electrospinning, some important parameters need to be discussed, including viscosity, surface tension, contact angle, conductivity, and dielectric constant. Viscosity is an essential characteristic

for producing fluids to be electrospun and the addition of polymer becomes imperative for this purpose since viscosity and surface tension are variables that depend on the selected polymer and its molecular weight, as well as the concentration ratio between solvent and polymer [38,75]. Although many studies highlight the importance of these characteristics for preparing fluids to be used in electrospinning, only a few present the results of analysis of these characteristics.

The PCL and PCL/zeolite 20% fluids prepared by Alp-Erbay et al. [69] had a viscosity of 0.7548 Pa·s and 8.194 Pa·s, respectively, that is, when zeolite was added to the polymer, the viscosity increased significantly. In addition, they analyzed the surface tension and conductivity of the fluids and the PCL had a surface tension of 27.8 mN/m, which was reduced to 24.0 mN/m when adding the zeolite. In terms of conductivity, zeolite had a minimal impact on the PCL solution's conductivity, with values in the 0.01-0.02 S/cm range.

Haghdoost et al. [71] also analyzed these parameters for the produced samples, and for viscosity found 0.050, 0.075, 0.675, 0.070, and 0.620 Pa·s for the N0 (PES), NZ10, NZ20, NB10, and NB20, respectively. The surface tension and conductivity of the fluids were 36 mN/m and 29 μS/cm for the N0, 32 mN/m and 20.30 μS/cm for the NZ10, 22 mN/m and 37.2 μS/cm for the NZ20, 30 mN/m and 18.2 μS/cm for the NB10, and 27.7 mN/m and 35.8 μS/cm for the NB20. Moreover, they also analyzed the contact angle of the fluid, and, as a result, the N0, NB20, and NZ20 had contact angles of 116.7º, 37.7º, and 32.5º, respectively.

These two studies were the only ones that carried out detailed analyses of fluid samples, however, some studies analyzed the contact angle. The Zeolite/PCDF fluid composite prepared by Kang & Kang [38] had a contact angle of ~125º, the M2' produced by He et al. [76] had a contact angle of 4.27º, and the PCL-PLA/Zeolite and PCL-

PLA/nHA/Zeolite fluid samples prepared by Mohandesnezhad et al. [70] had contact angles of 118º and 98º, respectively. Moreover, Sihombing et al. [36] studied the conductivity of the PS/Zeolite sample with 10% zeolite, and the result was a conductivity of 478 S·cm^{-1}.

Considering the scarcity of comprehensive analyses of the prepared solutions, the multitude of polymers employed, and the assortment of zeolite types utilized, conducting an extensive comparative assessment of these studies remains a challenge. Nevertheless, it is worth noting that certain studies have highlighted remarkable characteristics of these fluids.

According to Sreekumaret al. [77], obtaining uniform electrospun fibers from biopolymers requires relatively high viscosities, but excessively high viscosities can result in low processability due to instabilities during processing. Since lower levels of surface tension may boost the processability of biopolymers, lower surface tension is often favored during electrospinning, because it requires less effort to separate the variety of molecules during the applied electric field [78].

The conductivity of the solution greatly affects the electrospinning process and the fiber shape because the electrospinning solution repels, stretches, and forms the nanofibers. Therefore, by increasing the electrical conductivity of the solution as the jet becomes more strongly charged, a discernible decrease in the diameter of the nanofibers may be seen [79]. Moreover, it has been noted that adding salt to the polymer solution raised the charge on the electrospinning jet's surface, and the electrical forces drove the jet to lengthen and create uniform fibers with a lower diameter [37].

Unfortunately, it is not possible to make a deeper correlation regarding the synthesis with the properties of the materials due to the small number of studies available in the literature. However, although the properties of the solutions can help predict

processability problems during electrospinning, it is typically challenging to explain the influence of a single property without considering the impact of others and the target application field [69,81].

6.   ELECTROSPINNING PARAMETERS IN THE FABRICATION OF ZEOLITE COMPOSITE NANOFIBERS

As demonstrated in the preceding section, a wide array of polymers and materials can be incorporated into zeolites to craft composites suitable for a diverse range of applications. This section will review the electrospinning parameters employed, such as electric field strength, separation distance between the needle and collector, flow rate of the solution, voltage, fluid composition and solid concentration, and needle diameter. These parameters play a pivotal role in the manufacturing of these materials.

Figure 7 shows a typical electrospinning setup, with a straight plate, indicating some of the main processing components and factors, such as a syringe, distance, voltage, and collector. This setup was used by Anis & Hashaikeh [68] to obtain zeolite-Y/PVP fibers. In this case, the electrospun material was collected on an aluminum foil, and after electrospinning, the material was dried at 80 °C for 6 h to remove moisture. The material was then calcined at 550 °C for 2 h to remove the polymeric phase.
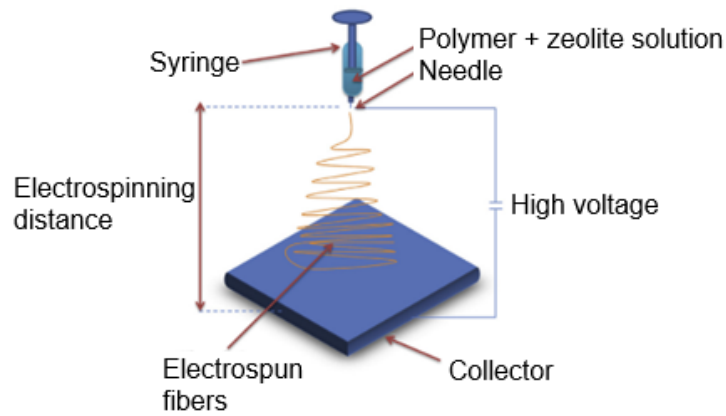
Figure 7. Schema of a generic electrospinning setup (Adapted from Anis & Hashaikeh, 2016). Copyright © 2016 Shaheen Fatima Anis,Raed Hashaikeh.

A scheme of the electrospinning device used by Sihombing et al. [36], which has a rotatory drum as a collector, is presented in Figure 8. To electrospun the zeolite/PVDF composite, they placed the mixture of PS and zeolite in a syringe with a 0.8 mm needle at 10 cm from the collector, with a flow rate of the solution of 13 µL/min at a voltage of 15 kV.
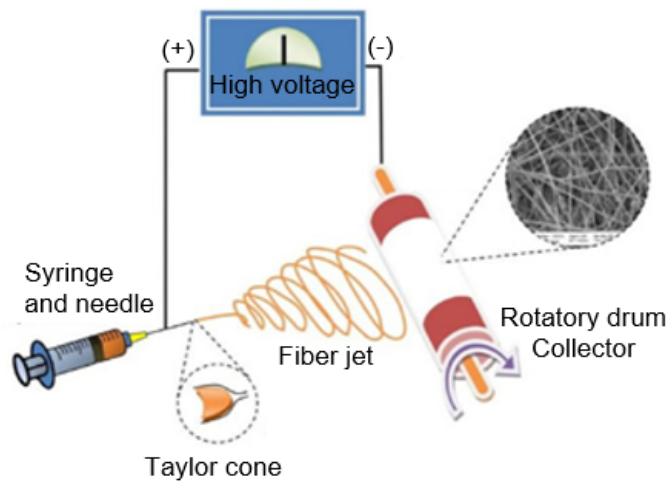
Figure 8. Illustration of the electrospinning device to produce a zeolite composite (Adapted from Sihombing et al., 2022). Copyright © 2022 Yuan Alfinsyah Sihombing et al.

The distance between the needle and the collector is important for determining the nanofiber's morphology, since the deposition time, the evaporation rate, and the

whipping or instability interval are dependent on this distance [27]. According to Huang et al. [81], when the distance between the needle and the collector is short, the spun fibers tend to stick to the collector and to each other, due to incomplete solvent evaporation. Table 2 illustrates a range of distances between the needle and the collector, spanning from 3 to 20 cm. Nevertheless, the most frequently utilized distances are consistently 10, 15, and 20 cm. While several studies omitted the specification of needle diameter, those that did provide this detail reported diameters within the range of 18 to 22 gauge. Notably, 20- and 21-gauge needles were the options most employed in the studies.

Concerning voltage, application of a high voltage from a power supply to the solution through a metallic needle induces a transformation of a spherical droplet into a characteristic Taylor cone shape. This electrical influence leads to the creation of ultrafine nanofibers, and the critical voltage required for this process varies depending on the specific polymer used [27]. By increasing voltage, it is possible to form nanofibers with smaller diameters, due to the stretching of the polymer solution around the charge repulsion within the polymer jet [82]. An increase in the applied voltage beyond the critical value will result in the formation of beads or beaded nanofibers, which is attributed to the decrease in the size of the Taylor cone and increase in jet velocity for the same flow rate [27]. In the studies examined, the voltage applied ranged from 10 to 30 kV and 20 kV was the most frequently employed voltage among these studies, as highlighted in Table 2.

Finally, the flow rate of the fluid is a very important parameter, since it is directly related to the fiber size, and can influence the fiber's porosity and morphology [82]. Since the flow rate directly affects nanofiber formation, a minimum flow rate is preferred to maintain a balance between the expelled polymeric solution and the replacement of that solution with a new one during jet formation [27]. Table 2 reveals a notable deviation

from standardization in terms of the flow rate parameter when compared to the other parameters. The flow rates utilized range from 0.1 to 3 ml/h, with the most frequently employed flow rate being 0.5 ml/h. This flow rate is relatively low, aligning with findings from the study conducted by Haider et al. [27].

Table 2. Electrospinning parameters for producing zeolite-based composites.

Composite	Flow rate (mL/h)	Voltage (kV)	Distance (cm)*	Needle (gauge)	Reference
PVA/NaX	0.5	20	14	-	[67]
Zeolite/PCDF	~3	10 – 12.5	3 – 20	-	[38]
Zeolite-Y fibers	0.5	10 – 28	10 – 15	20	[68]
Z-NaY/PVP (commercial)	0.5 – 3.5	20 – 25	15	20	[45]
Z-NaY/PVP (synthesized)					
Zeolite/PCL	3	14	15	20	[69]
nZH-Cu/ CNF	0.1	24	20	-	[43]
Zeolite/PCL-PLA	2	20 – 25	15	18	[70]
Zeolite/PCL-PLA/nHA					
MZ-8/PLA	1 – 2	20 – 30	15 – 20	-	[41]
NZ10	0.4 – 0.7	16	15	16 – 22	[71]
NZ20					
NB10					
NB20					
Zeolite/PS	~0.8	15	10	21	[36]
FZ30(20%)	0.5	14	20	-	[44]
FZ50(20%)					
FZ80(20%)					
M2'	0.01 μm/min	20	10	21	[72]
nZY/PG	1	20	20	21	[73]

Curc@ nZY-PG					
p(St-Co-AC)/Co-ZIF-67/C	0.6	18	10	-	[74]
ASC@ZSM-5/PCL-PEG/ DEX	1	25	20	22	[40]

* Distance between needle and collector

A zeolite/PVDF composite for simultaneous application in filtration and dehumidification was developed using the electrospinning technique by Kang and Kang [38]. The experimental electrospinning setup included a high-voltage source, a syringe pump, a metal needle, and a grounded collector. A syringe pump injected the composite into a metal needle, and a high-voltage source was connected to the tip of a metal needle and supplied the electrons to the composite. The tip-to-collector distance is one of the main variables in the electrospinning process that control the film morphology and porosity. A heat lamp was placed above the collector to speed evaporation of the solvents from the electrospun fibers.

Haghdoost et al. [71] produced a core-shell PES/PVP-zeolite, the solutions were placed into a 5 mL polyethylene syringe capped with a 22 G (core-shell PES) and 16 G (PVP/zeolite) inner and outer needle, respectively. A 33 × 11 cm aluminum foil was used as a collector, and the rate of the rotating collector was 100 rpm. After electrospinning, the fibers were placed in a desiccator for 24h, and thermal crosslinking was performed by placing the nanofibers in an oven at 200 °C for 1h. A schematic illustration of the electrospinning setup is presented in Figure 9.
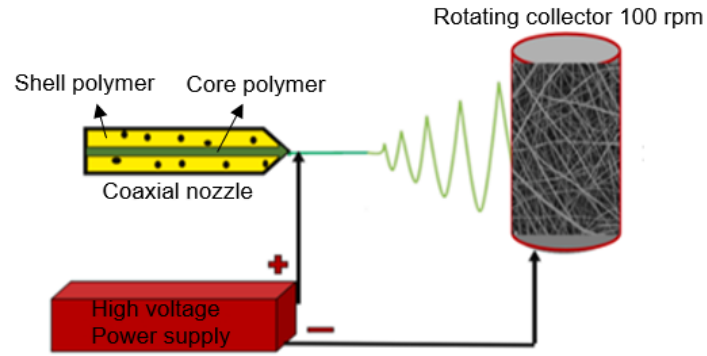
Figure 9. Schematic illustration of a core-shell electrospinning setup (adapted from Haghdoost et al., 2021). Copyright © 2021 Fatemeh Haghdoost, et al.

Zhang et al. [41] fabricated a MXene/ZIF-8/PLA membrane composite as an antibacterial nanofiber membrane by electrospinning. To do so, first a PLA solution was prepared using dichloromethane as a solvent, and the MXene/ZIF-8 suspension mixture was then added to the solution. As a result, the nanoparticles were encapsulated inside the fibrous membrane. Figure 10 displays the microstructure, offering a view of the encapsulated nanoparticles, along-with a photograph of the membrane.
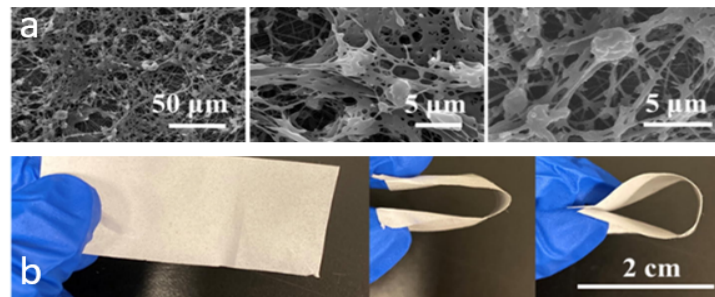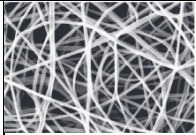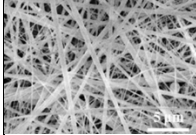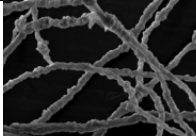
Figure 10. SEM images (a) and photographs (b) of a MZ-8/PLA membrane (adapted from Zhang et al., 2021). Copyright © 2021 Siqi Zhang et al.
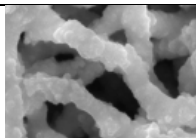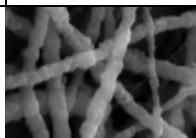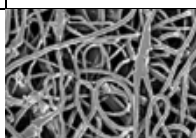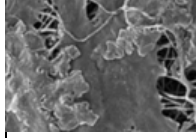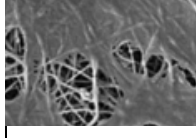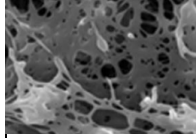
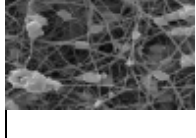Table 3 presents some characteristics of the nanofibrous composites investigated in this review, such as size, specific surface area, and pore size, as well as a pore volume scan, and SEM images for enhanced visualization, the composition of the cited materials
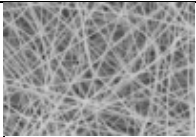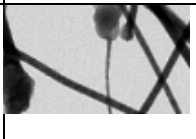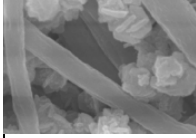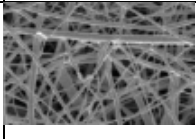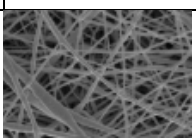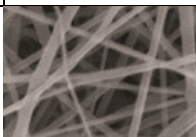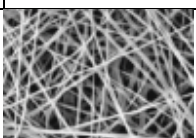
is presented in Table 1. However, it's worth noting that these characteristics do not appear to exhibit a clear correlation with each other.

In general, the diameter size of the fibers varies between ~50 nm and ~3μm, depending on the particle size of the zeolite. Some composites showed continuous fibers and others have small beads where the zeolite is encapsulated, as described by Zhang et al. [41]. Furthermore, there is no correspondence between the fibers diameter and surface area, being the surface area in the range 14.2 to 686 m^2/g. Although it did not present a pattern, some composites had porous characteristics, like those produced by Mofarrah et al. [40], Wu et al. [45], Jiang et al. [73], and He et al. [76], with pore sizes of 0.1 nm, 0.8 nm, 5.28 nm, and ~0.6 μm, respectively. Pore volumes of 0.06, 0.15, ~0.54, and ~0.24 cm³/g were obtained in the composites prepared by Mofarrah et al. [40], Cordero-Lanzac et al. [44], Jiang et al. [73], and Pahang et al. [74], respectively.

Table 3. Characteristics of the nanofibrous composites obtained.

Composite	SEM images[*©]	Fiber diameter (nm)	Specific surface area (m^2/g)	Reference
NaX /PVA		170	212	[67]
Zeolite/PCDF		350-400	-	[38]
Zeolite-Y fibers		~3000	686	[68]

Z-NaY/PVP (commercial)		750	192	[45]
Z-NaY/PVP (synthesized)		400	262	
Zeolite/PCL		773	-	[69]
nZH-Cu/CNF		1700 – 2400	-	[43]
Zeolite/PCL-PLA		-	-	[70]
Zeolite/PCL-PLA/nHA		-	-	
MZ-8/PLA		650	506.5	[41]
NZ10		2078	329.98	[71]
NZ20				
NB10		824	566.49	
NB20				

Zeolite/PS		-	-	[36]
FZ30(20%)		1240	421	[44]
M2'		-	-	[72]
nZY-PG		632	654	[73]
Curc@nZY-PG		64		
p(St-Co-AC)/Co-ZIF-67/C		232.25 – 414.29	39.5	[74]
DEX/ASC@ZSM-5/PCL-PEG		675	14.2	[40]

*All the images in this table are licensed for use by Elsevier and Copyright Clearance Center's RightsLink®

Thus, in terms of operational parameters, the optimal conditions for producing nanofibers with desirable properties involve maintaining a distance of 10-20 cm between the needle and the collector, using a needle diameter within the range of 18-22 gauge, applying a high voltage of approximately 20 kV, and adjusting the flow rate depending on the fluid viscosity.

7. APPLICATIONS, CHALLENGES, AND LIMITATIONS

The wide array of applications for the materials generated in the studies examined in this review is notably diverse, complicating the direct comparison of their conclusions. Nevertheless, it is important to highlight that the outcomes of the studies that tested these samples had highly promising results.

Pahang et al. [74] developed a method for extracting pesticide residues from foods, using a composite containing zeolitic-based metal-organic frameworks, chitosan, and, styrene-acrylonitrile copolymer, the composite was investigated in food samples including apples, tomatoes, honey, and milk and a pesticide recovery between 88.1–95.2 % was achieved, indicating that the fabricated composite is effective and promising for the pre-concentration of pesticides in various matrices.

After testing the electrospun PVP/zeolite sample for benzene adsorption, Wu et al. [45] concluded that the material presented a remarkably enhanced benzene adsorption of 667 mg/g and this is due to the synergistic effect of the hierarchical structures configured with porous PVP and microporous zeolite.

Rad et al. [67] tested the PVA/zeolite sample for the adsorption of Cd^{2+} and Ni^{2+} and found that the sample had a higher affinity for Cd^{2+} sorption than Ni^{2+} sorption. The best monolayer sorption capacities for Cd^{2+} and Ni^{2+} at 45 °C were 838.7 and 342.8 (mg g-1) at an equilibrium time of 60 min. Moreover, they also tested the reusability of the nanofibers, and the sample's capacity of adsorption did not change after five sorption-desorption cycles for both ions.

According to a study carried out by He et al. [72], a sample produced using a straightforward approach can operate as a cost-effective functional membrane to simultaneously remove bovine serum albumin, and NH_4^+ contaminants with a high solution flow in wastewater treatment.

The ZrO$_2$/HZSM-5 composites produced by Cordero-Lanzac et al. [44] were tested as catalysts in the dimethyl ether-to-olefins (DTO) process. As a result, they concluded that at a modest zeolite loading (5 wt%), at 400 °C, and a dimethyl ether partial pressure of 1 bar, the ZrO2/HZSM-5 catalysts demonstrated remarkable activity in the DTO process, attaining a maximum selectivity to olefins of around 70%.

Haghdoost et al. [71] produced an electrospun core-shell nanofiber sample for creatinine adsorption purposes, so to test the sample they removed creatinine from a solution and concluded that the removal of creatinine increased significantly with Beta zeolite and the highest adsorption potential of creatinine was obtained with the beta zeolite at a concentration of 20%. Moreover, by comparing the two types of zeolites that were tested, they showed that the zeolite particle size and surface area might be important factors in determining the functional impacts of core-shell nanofibers.

The biofilm samples produced by Vergara-Figueroa et al. [43] showed antimicrobial activity against two types of bacteria, *S. Typhi* and *S. aureus*, in *in vitro* tests confirming that they can be used as an antimicrobial barrier. Moreover, their biodegradable features would help lower contamination from the buildup of plastic garbage.

The *in vivo* and *in vitro* experiments performed by Zhang et al. [41] demonstrated that MZ-8/PLA can accelerate the healing of wounds infected with bacteria without evident resistance. A thorough analysis of its antibacterial abilities revealed that MZ-8 has bacterial inhibition rates of more than 99.0% against *Methicillin-resistant staphylococcus aureus* (MRSA) and *E. coli*. Additionally, MZ-8/PLA demonstrated strong photothermal and photodynamic therapy characteristics under near-infrared irradiation with bactericidal rates of up to 99.9% and 99.8% against *E. coli* and MRSA, respectively.

The samples produced by Alp-Erbay et al. [69], electrospun zeolite-containing PCL films, indicated a high ability to bind histamine after in vitro tests by *S. aureus* and *S. Paratyphi A*, even at the lowest mineral content. They attributed the results to the porous-like surface characteristics of the samples and their high selectivity for the adsorption of polar and hydrophilic molecules.

Sihombing et al. [36], who produced a PS/PNZ composite for desalination, tested the sample in artificial seawater and concluded that the sample with 30% zeolites had the best desalination results. The experiment demonstrates a strong potential for the future use of polystyrene/PNZ for desalination.

Jiang et al. [73] investigated the potential of the integration of Curcumin into zeolite Y/PCL-gelatin composites for glioblastoma post-surgical tumor resection via in vitro anticancer assays. They discovered that the integration of curcumin not only demonstrated superior cytotoxicity, effective anti-migratory activity, and enhanced apoptosis induction against glioblastoma cells in the first 72h but also demonstrated sustained and prolonged release of medicinal curcumin that can ensure an acceptable concentration of curcumin within the cells for a relatively long period to completely eradicate the remaining cancer cells after surgical tumor resection.

Mofarrah et al. [40] developed a zeolite (ZSM5)+PCL-PEG composite for the delivery of Dexamethasone (DEX) and ascorbic acid (ASC) to promote bone regeneration. The DEX/ASC@ZSM-5/PCL-PEG composite demonstrated successful continuous drug delivery over 2 weeks. Furthermore, the composite exhibited robust adhesion to human adipose-derived stem cells and elicited a positive impact on osteoblastic markers throughout an extended cell culture duration.

In general, the studies did not highlight the main challenges and limitations for zeolite-composite electrospinning production. However, Kang & Kang [38] related that

although there are advantages of the suberabsorbent polymers (SAPs) use as multi-functional filters produced with electrospinning, the synthesis has some limitations due to the complex processes, expensive equipment and material cost that are considered critical obstacles for the production.

Xue et al. [35] pointed out that the simulation models related to the electrospinning process need to be optimized by considering all of the properties of the liquid used for electrospinning and processing parameters, to better elucidate the phenomenology of the electrified jets. Then, the theoretical models should be realistic to predict the behavior of the electrified jet to produce well-controlled size, structure, and morphology.

Furthermore, they also commented on the large amount of solvents involved, which results in both economic and environmental concerns, hence, it is important to develop methods that use "green" solvents or even solvent-free systems, though this issue is more related to the polymer than the electrospinning itself, since in the study carried out by Rad et al. [67] the solvent used was water. And finally, the challenge remains to produce nanofibers with diameters below 10 nm [35].

Lastly, Table 4 presents a summary of the applications, results and conclusions of the studies that tested the production of electrospun material.

Table 4. Application, results, and conclusion of the electrospun materials

Composite	Application	Results	Conclusions	Reference
PVA/NaX	Ni^{2+} and Cd^{2+} removal from aqueous solution	Monolayer sorption capacities for Cd^{2+} and Ni^{2+} were 838.7 and 342.8 (mg g-1).	The adsorption capacity of the composite did not change after 5 adsorption-desorption cycles, confirming the reusability of the material.	[67]
Z-NaY/PVP (commercial)	Benzene adsorption	Benzene adsorption of 667 mg/g.	The significantly enhanced adsorption is due to the synergistic effect of the hierarchical structures configured with porous PVP and microporous zeolite.	[45]
Z-NaY/PVP (synthesized)	Histamine-binding	The composite presented high ability to bind histamine, through in vitro tests by *S. aureus* and *S. Paratyphi A.*	Even at the lowest mineral content the material had excellent results, which can be related to the porous-like surface characteristics of the samples, and their high selectivity for the adsorption of polar and hydrophilic molecules.	[69]
Zeolite/PCL	Antimicrobial barrier	The in-vitro tests confirmed that it can be used as an antimicrobial barrier.	The biodegradable features can aid in lowering contamination issues brought on by the buildup of plastic garbage.	[43]
Zeolite/PCL-PLA	Bacterial infections	The material presented antibacterial abilities revealed that MZ-8 has bacterial inhibition rates of more than 99.0% against (MRSA) and *E. coli.*	The composite can accelerate the healing of wounds infected with bacteria without evident resistance.	[41]

Zeolite/PCL-PLA/nHA	Creatinine adsorption	The removal of creatinine increased significantly with Beta zeolite and the highest adsorption potential of creatinine was obtained with the beta zeolite in concentration of 20%.	The zeolite particle size and surface area might be important factors in determining the functional impacts of core-shell nanofibers.	[71]
MZ-8/PLA	Desalination	In artificial seawater the sample with 30% zeolites had the best results when desalinating	The experiment demonstrates that there is strong potential for the future use of polystyrene/PNZ in desalination.	[36]
NZ10	Catalysis (dimethyl ether-to-olefins process)	Maximum selectivity to olefins of around 70%.	With modest zeolite loading the catalysts demonstrated significant activity.	[44]
NZ20	Adsorption/separation membranes in organic carbon interception, Ammonium recovery	The maximum experimental adsorption capacity achieved was 27.02 mg/g, in the static adsorption process.	The sample produced can operate as a cost-effective functional membrane to remove bovine serum albumin, and NH_4^+ contaminants simultaneously with a high solution flow in wastewater treatment.	[72]
NB10	Postsurgical glioblastoma treatment	The integration of curcumin demonstrated superior cytotoxicity, effective anti-migratory activity, and enhanced apoptosis induction against glioblastoma cells in the first 72h.	The material also presented a sustained and prolonged release of medicinal curcumin that can ensure an acceptable concentration of curcumin within the cells for a relatively long period to completely eradicate the remaining cancer cells after surgical tumor resection.	[73]

NB20	Pesticide residue analysis in food samples	Pesticide recovery between 88.1–95.2 %.	The composite is effective and can be promising for pre-concentration of pesticides in various matrices.	[74]
Zeolite/PS	Dexamethasone and and ascorbic acid delivery for bone regeneration	The composite delivered the drug continuously over 2 weeks.	The composite showed strong adhesion to the cell and proliferation for human adipose-derived stem cells and a favorable effect on osteoblastic markers throughout a long-term cell culture.	[40]

8. CONCLUDING REMARKS

Electrospinning has emerged as a highly promising technique for the fabrication of zeolite/polymer composite nanofibers, primarily due to its versatility and cost-effectiveness. This synthesis procedure allows the creation of composites with predefined porosity and surface area, offering control over the morphology of the resulting nanofibers. Several parameters, including component concentration, fluid viscosity, applied voltage, tip-to-collector distance, the needle, and solvent, significantly impact the final product. It's noteworthy that these parameters play a crucial role in the preparation of fluids for electrospinning, which is essential for the reproducibility of studies, although only a limited number of studies have presented these essential details. By mastering these parameters, it becomes feasible to tailor electrospun nanofibers to fulfill a wide range of functions.

Electrospun zeolite/polymer composite nanofibers have potential applications in various fields, encompassing filtration, dentistry, medicine, and catalysis. Consequently, these electrospun nanofibrous membranes and their composites not only hold great promise for various industrial applications but have also presented promising results. Given the diversity of applications, a comprehensive analysis of material performance across these applications remains challenging, preventing direct comparisons of results. Nevertheless, it is essential to recognize that these materials have proven to be efficient in their specific applications, highlighting the potential of electrospun nanofibers to address multifaceted challenges in various industries.

It has been shown that electrospinning is a simple, economical, and relatively novel way to develop zeolite/polymer composite nanofibers with hierarchical porosity and, depending on the operating conditions and type of polymer, different materials can be produced. In addition to these operating parameters, the precursor solution is also of

paramount importance, and several polymers to prepare it are available as have been shown (PVDF, PVP, polyvinyl alcohol, polycaprolactone, polylactic acid, polyurethane, poly(methyl methacrylate, PEG, among others). Depending on the precursor solution viscosity and the desired properties of the final materials, the operation conditions are selected. The present review has shown that the most usual parameters to obtain adequate nanofibers involve maintaining a distance of 10-20 cm between the needle and the collector, using a needle diameter within the range of 18-22 gauge, applying a high voltage of approximately 20 kV, and adjusting the flow rate depending on the fluid viscosity.

DECLARATION OF COMPETING INTEREST

The authors declare that they have no known competing financial interests or personal relationships that could have appeared to influence the work reported in this paper.

DATA AVAILABILITY

Data will be made available on request.

REFERENCES

[1]   G.S. Souza, Desenvolvimento de compósito zeólita Na-LTA/polidimetilsiloxano aplicado para separação CO2/N2 por <mark>adsorção.</mark> Federal University of Santa Catarina, 2021.

[2]   K. Byrappa, M. Yoshimura, Hydrothermal Synthesis and Growth of Zeolites, Handbook of Hydrothermal Technology. (2013) 269–347. https://doi.org/10.1016/B978-0-12-375090-7.00006-2.

[3]   W.C. Wong, L.T.Y. Au, P.P.S. Lau, C.T. Ariso, K.L. Yeung, Effects of synthesis parameters on the zeolite membrane morphology, J Memb Sci. 193 (2001) 141–161. https://doi.org/10.1016/S0376-7388(01)00454-9.

[4]   A.R. Da Silveira, Desenvolvimento de materiais compósitos geopolímero-zeólita derivados de resíduos industriais para adsorção de CO_2, Federal University of Santa Catarina, 2021.

[5]   A.L. Freire, C.D. Moura-Nickel, G. Scaratti, A. De Rossi, M.H. Araújo, A. De Noni Júnior, A.E. Rodrigues, E.R. Castellón, R. de Fátima Peralta Muniz Moreira, Geopolymers produced with fly ash and rice husk ash applied to CO2 capture, J Clean Prod. 273 (2020). https://doi.org/10.1016/j.jclepro.2020.122917.

[6]   M.R. Oliveira, J.A. Cecilia, D. Ballesteros-Plata, I. Barroso-Martín, P. Núñez, A. Infantes-Molina, E. Rodríguez-Castellón, Microwave-Assisted Synthesis of Zeolite A from Metakaolinite for CO2 Adsorption, Int J Mol Sci. 24 (2023) 14040. https://doi.org/10.3390/ijms241814040.

[7]   S. Su, H. Ma, X. Chuan, Hydrothermal synthesis of zeolite A from K-feldspar and its crystallization mechanism, Advanced Powder Technology. 27 (2016) 139–144. https://doi.org/10.1016/j.apt.2015.11.011.

[8]   M. Minelli, E. Papa, V. Medri, F. Miccio, P. Benito, F. Doghieri, E. Landi, Characterization of novel geopolymer – Zeolite composites as solid adsorbents for CO2 capture, Chemical Engineering Journal. 341 (2018) 505–515. https://doi.org/10.1016/j.cej.2018.02.050.

[9]   K. Pasupathy, S. Ramakrishnan, J. Sanjayan, Formulating eco-friendly geopolymer foam concrete by alkali-activation of ground brick waste, J Clean Prod. 325 (2021) 129180. https://doi.org/10.1016/j.jclepro.2021.129180.

[10] H.S. Hassan, H.A. Abdel-Gawwad, S.R.V. García, I. Israde-Alcántara, Fabrication and characterization of thermally-insulating coconut ash-based geopolymer foam, Waste Management. 80 (2018) 235–240. https://doi.org/10.1016/j.wasman.2018.09.022.

[11] S. Onutai, S. Jiemsirilers, P. Thavorniti, T. Kobayashi, Fast microwave syntheses of fly ash based porous geopolymers in the presence of high alkali concentration, Ceram Int. 42 (2016) 9866–9874. https://doi.org/10.1016/j.ceramint.2016.03.086.

[12] A.T. Pinto, Introdução ao Estudo dos Geopolimeros, Universidade de Trás-Os-Montes e Alto Douro. 28 (2006) 423.

[13] T. Kovářík, J. Hájek, M. Pola, D. Rieger, M. Svoboda, J. Beneš, P. Šutta, K. Deshmukh, V. Jandová, Cellular ceramic foam derived from potassium-based geopolymer composite: Thermal, mechanical and structural properties, Mater Des. 198 (2021). https://doi.org/10.1016/j.matdes.2020.109355.

[14] D. Medpelli, R. Sandoval, L. Sherrill, K. Hristovski, D.-K. Seo, Iron oxide-modified nanoporous geopolymers for arsenic removal from ground water, Resource-Efficient Technologies. 1 (2015) 19–27. https://doi.org/10.1016/j.reffit.2015.06.007.

[15] K. Okada, A. Imase, T. Isobe, A. Nakajima, Capillary rise properties of porous geopolymers prepared by an extrusion method using polylactic acid (PLA) fibers as the pore formers, J Eur Ceram Soc. 31 (2011) 461–467. https://doi.org/10.1016/j.jeurceramsoc.2010.10.035.

[16] E. Papa, E. Landi, A.N. Murri, F. Miccio, A. Vaccari, V. Medri, CO2 adsorption at intermediate and low temperature by geopolymer-hydrotalcite composites, Open Ceramics. 5 (2021) 100048. https://doi.org/10.1016/j.oceram.2020.100048.

[17] E. Papa, V. Medri, P. Benito, A. Vaccari, S. Bugani, J. Jaroszewicz, E. Landi, Insights into the macroporosity of freeze-cast hierarchical geopolymers, RSC Adv. 6 (2016) 24635–24644. https://doi.org/10.1039/c6ra02232d.

[18] S.N. Zailan, N. Mahmed, M.M.A.B. Abdullah, A.V. Sandu, Self-cleaning geopolymer concrete - A review, in: IOP Conf Ser Mater Sci Eng, Institute of Physics Publishing, 2016. https://doi.org/10.1088/1757-899X/133/1/012026.

[19] A.L. Freire, H.J. José, R. de Fátima Peralta Muniz Moreira, Potential applications for geopolymers in carbon capture and storage, International Journal of Greenhouse Gas Control. 118 (2022). https://doi.org/10.1016/j.ijggc.2022.103687.

[20] H. Chen, Y.J. Zhang, P.Y. He, C.J. Li, L.C. Liu, Novel activated carbon route to low-cost geopolymer based porous composite with high mechanical resistance and enhanced CO2

capacity, Microporous and Mesoporous Materials. 305 (2020) 110282. https://doi.org/10.1016/j.micromeso.2020.110282.

[21]   M. Minelli, V. Medri, E. Papa, F. Miccio, E. Landi, F. Doghieri, Geopolymers as solid adsorbent for CO2 capture, Chem Eng Sci. 148 (2016) 267–274. https://doi.org/10.1016/j.ces.2016.04.013.

[22]   S.H. Bong, M. Xia, B. Nematollahi, C. Shi, Ambient temperature cured 'just-add-water' geopolymer for 3D concrete printing applications, Cem Concr Compos. 121 (2021) 104060. https://doi.org/10.1016/j.cemconcomp.2021.104060.

[23]   B. Panda, S.C. Paul, L.J. Hui, Y.W.D. Tay, M.J. Tan, Additive manufacturing of geopolymer for sustainable built environment, J Clean Prod. 167 (2017) 281–288. https://doi.org/10.1016/j.jclepro.2017.08.165.

[24]   S. Muthukrishnan, S. Ramakrishnan, J. Sanjayan, Effect of microwave heating on interlayer bonding and buildability of geopolymer 3D concrete printing, Constr Build Mater. 265 (2020) 120786. https://doi.org/10.1016/j.conbuildmat.2020.120786.

[25]   A. Khalil, R. Hashaikeh, N. Hilal, 3D printed zeolite-Y for removing heavy metals from water, Journal of Water Process Engineering. 42 (2021) 102187. https://doi.org/10.1016/j.jwpe.2021.102187.

[26]   M. Etxeberria-Benavides, T. Johnson, S. Cao, B. Zornoza, J. Coronas, J. Sanchez-Lainez, A. Sabetghadam, X. Liu, E. Andres-Garcia, F. Kapteijn, J. Gascon, O. David, PBI mixed matrix hollow fiber membrane: Influence of ZIF-8 filler over H2/CO2 separation performance at high temperature and pressure, Sep Purif Technol. 237 (2020). https://doi.org/10.1016/j.seppur.2019.116347.

[27]   A. Haider, S. Haider, I.K. Kang, A comprehensive review summarizing the effect of electrospinning parameters and potential applications of nanofibers in biomedical and biotechnology, Arabian Journal of Chemistry. 11 (2018) 1165–1188. https://doi.org/10.1016/j.arabjc.2015.11.015.

[28]   A.L. Yarin, S. Koombhongse, D.H. Reneker, Taylor cone and jetting from liquid droplets in electrospinning of nanofibers, J Appl Phys. 90 (2001) 4836–4846. https://doi.org/10.1063/1.1408260.

[29]   B.A. da Silva, R. de S. Cunha, A. Valério, A.D.N. Junior, D. Hotza, S.Y.G. González, Electrospinning of cellulose using ionic liquids: An overview on processing and applications, Eur Polym J. 147 (2021). https://doi.org/10.1016/j.eurpolymj.2021.110283.

[30] M. Calzado-Delgado, M.O. Guerrero-Pérez, K.L. Yeung, A new versatile x–y–z electrospinning equipment for nanofiber synthesis in both far and near field, Sci Rep. 12 (2022) 1–9. https://doi.org/10.1038/s41598-022-08310-0.

[31] A.L. Yarin, S. Koombhongse, D.H. Reneker, Bending instability in electrospinning of nanofibers, J Appl Phys. 89 (2001) 3018–3026. https://doi.org/10.1063/1.1333035.

[32] B. Fu, X. Zhou, Y. Wang, High-rate performance electrospun Na0.44MnO2 nanofibers as cathode material for sodium-ion batteries, J Power Sources. 310 (2016) 102–108. https://doi.org/10.1016/j.jpowsour.2016.01.101.

[33] Q. Zhang, D. Jia, Z. Yang, X. Duan, Q. Chen, Y. Zhou, Synthesis of novel cobalt-containing polysilazane nanofibers with fluorescence by electrospinning, Polymers (Basel). 8 (2016). https://doi.org/10.3390/polym8100350.

[34] X. Zhang, J. Chen, Y. Zeng, Morphology development of helical structure in bicomponent fibers during spinning process, Polymer (Guildf). 201 (2020). https://doi.org/10.1016/j.polymer.2020.122609.

[35] J. Xue, T. Wu, Y. Dai, Y. Xia, Electrospinning and electrospun nanofibers: Methods, materials, and applications, Chem Rev. 119 (2019) 5298–5415. https://doi.org/10.1021/acs.chemrev.8b00593.

[36] Y.A. Sihombing, M.Z.E. Sinaga, R. Hardiyanti, Susilawati, I.R. Saragi, Rangga, Preparation, characterization, and desalination study of polystyrene membrane integrated with zeolite using the electrospinning method, Heliyon. 8 (2022). https://doi.org/10.1016/j.heliyon.2022.e10113.

[37] J. Tang, X. Liu, X. Chang, X. Ji, W. Zhou, Elastic geopolymer based on nanotechnology: Synthesis, characterization, properties, and applications, Ceram Int. 48 (2022) 5965–5971. https://doi.org/10.1016/j.ceramint.2021.11.070.

[38] D.H. Kang, H.W. Kang, Surface energy characteristics of zeolite embedded PVDF nanofiber films with electrospinning process, Appl Surf Sci. 387 (2016) 82–88. https://doi.org/10.1016/j.apsusc.2016.06.096.

[39] Y. Hu, Y. Xu, R.L. Mintz, X. Luo, Y. Fang, Y.H. Lao, H.F. Chan, K. Li, S. Lv, G. Chen, Y. Tao, Y. Luo, M. Li, Self-intensified synergy of a versatile biomimetic nanozyme and doxorubicin on electrospun fibers to inhibit postsurgical tumor recurrence and metastasis, Biomaterials. 293 (2023). https://doi.org/10.1016/j.biomaterials.2022.121942.

[40] M. Mofarrah, D. Jafari-Gharabaghlou, M. Dadashpour, N. Zarghami, Fabricating ZSM-5 zeolite/ polycaprolactone nano-fibers co-loaded with dexamethasone and ascorbic acid:

Potential application in osteogenic differentiation of human adipose-derived stem cells, J Drug Deliv Sci Technol. 79 (2023). https://doi.org/10.1016/j.jddst.2022.103999.

[41] S. Zhang, J. Ye, X. Liu, Y. Wang, C. Li, J. Fang, B. Chang, Y. Qi, Y. Li, G. Ning, Titanium carbide/zeolite imidazole framework-8/polylactic acid electrospun membrane for near-infrared regulated photothermal/photodynamic therapy of drug-resistant bacterial infections, J Colloid Interface Sci. 599 (2021) 390–403. https://doi.org/10.1016/j.jcis.2021.04.109.

[42] X. Shan, J. Lu, Q. Wu, Z. Sun, X. Zhang, C. Li, S. Yang, H. Li, L. Tian, Solid-state electrochemiluminescence sensor based on the carbon fibers derived from ZIFs-containing electrospun fibers for chlorpyrifos detection, Microchemical Journal. 185 (2023). https://doi.org/10.1016/j.microc.2022.108221.

[43] J. Vergara-Figueroa, S. Alejandro-Martin, F. Cerda-Leal, W. Gacitúa, Dual electrospinning of a nanocomposites biofilm: Potential use as an antimicrobial barrier, Mater Today Commun. 25 (2020). https://doi.org/10.1016/j.mtcomm.2020.101671.

[44] M.O. Guerrero-Pérez, Research Progress on the applications of electrospun nanofibers in catalysis, Catalysts 12(1) (2022) 9. https://doi.org/10.3390/catal12010009

[45] X. Wu, X. Yang, H. Yang, Z. Guo, J. Lin, W. Wu, X. Liang, Y. He, Hierarchically structured PVP porous fibers derived from the embedding of NaY zeolite synergize the adsorption of benzene, Compos B Eng. 179 (2019). https://doi.org/10.1016/j.compositesb.2019.107542.

[46] J.A. Nollet, Part of a letter from Abbè Nollet, of the Royal Academy of Science at Paris, and F. R. S. to Martin Folkes Esq; President of the same, concerning electricity, Philos Trans R Soc Lond. 45 (1748) 187–194. https://doi.org/10.1098/rstl.1748.0018.

[47] Lord Rayleigh, On the equilibrium of liquid conducting masses charged with electricity, The London, Edinburgh, and Dublin Philosophical Magazine and Journal of Science. 14 (1882) 184–186. https://doi.org/10.1080/14786448208628425.

[48] J.F. Cooley, Apparatus for electrically dispersing fluids., US692631A, 1902.

[49] W.J. Morton, Method of dispersing fluids., 705691, 1902.

[50] A. Formhals, Process and apparatus for preparing artificial threads, 1975504, 1934.

[51] A. Formhals, Method and apparatus for spinning, 2349950, 1944.

[52] G.I. Taylor, Electrically driven jets, Proceedings of the Royal Society of London. A. Mathematical and Physical Sciences. 313 (1969) 453–475. https://doi.org/10.1098/rspa.1969.0205.

[53] G.I. Taylor, The force exerted by an electric field on a long cylindrical conductor, Proc R Soc Lond A Math Phys Sci. 291 (1966) 145–158. https://doi.org/10.1098/rspa.1966.0085.

[54] G.I. Taylor, Disintegration of water drops in an electric field, Proc R Soc Lond A Math Phys Sci. 280 (1964) 383–397. https://doi.org/10.1098/rspa.1964.0151.

[55] H. Fong, I. Chun, D.H. Reneker, Beaded nanofibers formed during electrospinning, Polymer (Guildf). 40 (1999) 4585–4592. https://doi.org/10.1016/S0032-3861(99)00068-3.

[56] M.M. Hohman, M. Shin, G. Rutledge, M.P. Brenner, Electrospinning and electrically forced jets. I. Stability theory, Physics of Fluids. 13 (2001) 2201–2220. https://doi.org/10.1063/1.1383791.

[57] Y.M. Shin, M.M. Hohman, M.P. Brenner, G.C. Rutledge, Electrospinning: A whipping fluid jet generates submicron polymer fibers, Appl Phys Lett. 78 (2001) 1149–1151. https://doi.org/10.1063/1.1345798.

[58] D.H. Reneker, A.L. Yarin, H. Fong, S. Koombhongse, Bending instability of electrically charged liquid jets of polymer solutions in electrospinning, J Appl Phys. 87 (2000) 4531–4547. https://doi.org/10.1063/1.373532.

[59] C.S. Cundy, P.A. Cox, The hydrothermal synthesis of zeolites: Precursors, intermediates and reaction mechanism, Microporous and Mesoporous Materials. 82 (2005) 1–78. https://doi.org/10.1016/j.micromeso.2005.02.016.

[60] A.B. Luz, Zeólitas: propriedades e usos industriais, in: F.F. Lins (Ed.), Série Tecnologia Mineral, CETEM/CNPq, 1995: p. 35. http://mineralis.cetem.gov.br:8080/bitstream/cetem/132/1/stm-68.pdf.

[61] B. Haider, M.R. Dilshad, M.A.U. Rehman, J.V. Schmitz, M. Kaspereit, Highly permeable novel PDMS coated asymmetric polyethersulfone membranes loaded with SAPO-34 zeoilte for carbon dioxide separation, Sep Purif Technol. 248 (2020). https://doi.org/10.1016/j.seppur.2020.116899.

[62] G. Franchin, P. Colombo, Porous geopolymer components through inverse replica of 3D printed sacrificial templates, Journal of Ceramic Science and Technology. 6 (2015) 105–112. https://doi.org/10.4416/JCST2014-00057.

[63] M. Chougan, S.H. Ghaffar, M. Jahanzat, A. Albar, N. Mujaddedi, R. Swash, The influence of nano-additives in strengthening mechanical performance of 3D printed multi-binder geopolymer composites, Constr Build Mater. 250 (2020) 118928. https://doi.org/10.1016/j.conbuildmat.2020.118928.

[64] J.H. Lim, B. Panda, Q.C. Pham, Improving flexural characteristics of 3D printed geopolymer composites with in-process steel cable reinforcement, Constr Build Mater. 178 (2018) 32–41. https://doi.org/10.1016/j.conbuildmat.2018.05.010.

[65] S. Muthukrishnan, S. Ramakrishnan, J. Sanjayan, Effect of alkali reactions on the rheology of one-part 3D printable geopolymer concrete, Cem Concr Compos. 116 (2021) 103899. https://doi.org/10.1016/j.cemconcomp.2020.103899.

[66] B. Panda, S.C. Paul, M.J. Tan, Anisotropic mechanical performance of 3D printed fiber reinforced sustainable construction material, Mater Lett. 209 (2017) 146–149. https://doi.org/10.1016/j.matlet.2017.07.123.

[67] L.R. Rad, A. Momeni, B.F. Ghazani, M. Irani, M. Mahmoudi, B. Noghreh, Removal of Ni2+ and Cd2+ ions from aqueous solutions using electrospun PVA/zeolite nanofibrous adsorbent, Chemical Engineering Journal. 256 (2014) 119–127. https://doi.org/10.1016/j.cej.2014.06.066.

[68] S.F. Anis, R. Hashaikeh, Electrospun zeolite-Y fibers: Fabrication and morphology analysis, Microporous and Mesoporous Materials. 233 (2016) 78–86. https://doi.org/10.1016/j.micromeso.2015.11.022.

[69] E. Alp-Erbay, K.J. Figueroa-Lopez, J.M. Lagaron, E. Çağlak, S. Torres-Giner, The impact of electrospun films of poly(ε-caprolactone) filled with nanostructured zeolite and silica microparticles on in vitro histamine formation by Staphylococcus aureus and Salmonella Paratyphi A, Food Packag Shelf Life. 22 (2019). https://doi.org/10.1016/j.fpsl.2019.100414.

[70] S. Mohandesnezhad, Y. Pilehvar-Soltanahmadi, E. Alizadeh, A. Goodarzi, S. Davaran, M. Khatamian, N. Zarghami, M. Samiei, M. Aghazadeh, A. Akbarzadeh, In vitro evaluation of Zeolite-nHA blended PCL/PLA nanofibers for dental tissue engineering, Mater Chem Phys. 252 (2020). https://doi.org/10.1016/j.matchemphys.2020.123152.

[71] F. Haghdoost, S.H. Bahrami, J. Barzin, A. Ghaee, Preparation and characterization of electrospun polyethersulfone/polyvinylpyrrolidone-zeolite core–shell composite nanofibers for creatinine adsorption, Sep Purif Technol. 257 (2021). https://doi.org/10.1016/j.seppur.2020.117881.

[72] W. He, M. Zhang, H. Du, A. Amrane, H. Yu, Y. Liu, Anchoring nano-zeolite NaX particles on polydopamine-modified PVDF/PAN electrospun membranes for enhancing interception, adsorption and antifouling performance, Colloids Surf A Physicochem Eng Asp. 670 (2023). https://doi.org/10.1016/j.colsurfa.2023.131587.

[73] B. Jiang, Z. Yang, H. Shi, A. Turki Jalil, M. Mahmood Saleh, W. Mi, Potentiation of Curcumin-loaded zeolite Y nanoparticles/PCL-gelatin electrospun nanofibers for postsurgical glioblastoma treatment, J Drug Deliv Sci Technol. 80 (2023). https://doi.org/10.1016/j.jddst.2022.104105.

[74] F. Pahang, S. Amini, H. Ebrahimzadeh, S.H. Kandeh, Electrospun poly(ST-Co-AC)/Co-ZIF-67@Chitosan composite nanofibers as a sorbent with superior reusability for pesticide residues analysis in food samples, Microchemical Journal. 188 (2023). https://doi.org/10.1016/j.microc.2023.108476.

[75] J. Liu, G. Jiang, Y. Liu, J. Di, Y. Wang, Z. Zhao, Q. Sun, C. Xu, J. Gao, A. Duan, J. Liu, Y. Wei, Y. Zhao, L. Jiang, Hierarchical macro-meso-microporous ZSM-5 zeolite hollow fibers with highly efficient catalytic cracking capability, Sci Rep. 4 (2014). https://doi.org/10.1038/srep07276.

[76] H. He, P. Xu, T. Shang, S. Wang, M. Jiang, X. Yue, Fabrication of a flexible and efficient electromagnetic wave absorber based on reduced graphene oxide/Fe7Co3 filled into polydimethylsiloxane, Synth Met. 293 (2023) 117296. https://doi.org/10.1016/j.synthmet.2023.117296.

[77] S. Sreekumar, P. Lemke, B.M. Moerschbacher, S. Torres-Giner, J.M. Lagaron, Preparation and optimization of submicron chitosan capsules by water-based electrospraying for food and bioactive packaging applications, Food Addit Contam Part A Chem Anal Control Expo Risk Assess. 34 (2017) 1795–1806. https://doi.org/10.1080/19440049.2017.1347284.

[78] X. Geng, O.H. Kwon, J. Jang, Electrospinning of chitosan dissolved in concentrated acetic acid solution, Biomaterials. 26 (2005) 5427–5432. https://doi.org/10.1016/j.biomaterials.2005.01.066.

[79] S. Kim, J. Kirch, L. Mawst, Highly strained InAs quantum wells on InP substrates for mid-IR emission, J Cryst Growth. 312 (2010) 1388–1390. https://doi.org/10.1016/j.jcrysgro.2009.12.003.

[80] S. Torres-Giner, S. Wilkanowicz, B. Melendez-Rodriguez, J.M. Lagaron, Nanoencapsulation of Aloe vera in Synthetic and Naturally Occurring Polymers by Electrohydrodynamic Processing of Interest in Food Technology and Bioactive Packaging, J Agric Food Chem. 65 (2017) 4439–4448. https://doi.org/10.1021/acs.jafc.7b01393.

[81] Z.M. Huang, Y.Z. Zhang, M. Kotaki, S. Ramakrishna, A review on polymer nanofibers by electrospinning and their applications in nanocomposites, Compos Sci Technol. 63 (2003) 2223–2253. https://doi.org/10.1016/S0266-3538(03)00178-7.

[82] T.J. Sill, H.A. von Recum, Electrospinning: Applications in drug delivery and tissue engineering, Biomaterials. 29 (2008) 1989–2006. https://doi.org/10.1016/j.biomaterials.2008.01.011.

[83] S.F. Anis, A. Khalil, Saepurahman, G. Singaravel, R. Hashaikeh, A review on the fabrication of zeolite and mesoporous inorganic nanofibers formation for catalytic applications, Micropor Mesopor Mat. 236 (2016) 176-192. https://doi.org/10.1016/j.micromeso.2016.08.043.